We are IntechOpen, the world's leading publisher of Open Access books Built by scientists, for scientists

6,900
Open access books available

186,000
International authors and editors

200M
Downloads

Our authors are among the

154
Countries delivered to

TOP 1%
most cited scientists

12.2%
Contributors from top 500 universities

CLARIVATE ANALYTICS
BOOK CITATION INDEX
INDEXED

WEB OF SCIENCE™

Selection of our books indexed in the Book Citation Index
in Web of Science™ Core Collection (BKCI)

Interested in publishing with us?
Contact book.department@intechopen.com

Numbers displayed above are based on latest data collected.
For more information visit www.intechopen.com

Characterization of Metamaterial Transmission Lines with Coupled Resonators Through Parameter Extraction

Francisco Aznar-Ballesta[1], Marta Gil[2], Miguel Durán-Sindreu[3],
Jordi Bonache[3] and Ferran Martín[3]
[1]Universidad Politécnica de Madrid,
[2]Universidad de Castilla-La Mancha,
[3]Universitat Autònoma de Barcelona,
Spain

1. Introduction

Since resonant-type metamaterial transmission lines were proposed (Martín et al., 2003), this kind of transmission lines have been of significant importance in the development of new and innovative microwave devices. The small size and novel characteristics of these transmission lines based on sub-wavelength resonators allows the miniaturization and improvement of existing devices (Bonache et al., 2006a, 2006b; Gil et al., 2007a, 2007b), as well as the design of components with new functionalities (Sisó et al., 2008, 2009). Due to the complicated layouts that these designs usually involve, having an accurate equivalent circuit model is an important assist during the design process. Besides, the application of parameter extraction methods (Bonache et al., 2006c) to obtain the values of the electrical parameters of the circuit model makes possible the characterization of both the transmission line and, therefore, the microwave device. The circuit models and parameter extraction methods presented in this chapter have been widely verified and their accuracy permits even their application for automatic layout generation based on space mapping techniques (Selga et al., 2010), which is a large and useful advance in the design of such structures.

2. Metamaterial transmission lines based on the resonant approach

In this section, several structures of metamaterial transmission lines based on the resonant approach are shown. The considered structures are implemented in planar technology and consist in a host microstrip line or in coplanar wave guide (CPW) loaded with sub-wavelength resonant particles. Each structure requires the combination of resonators and other loading elements in order to achieve the intended propagation. In the following sections, several structures based on different kinds of resonators are presented and discussed.

2.1 Transmission lines based on Split-Ring Resonators (SRRs)

The metamaterial transmission lines based on SRRs were proposed in 2003 by Martín et al. (Martín et al., 2003). They designed a transmission line exhibiting left-handed transmission

by loading a CPW structure with SRRs. Left-handed transmission is achieved when the effective permittivity and permeability of a medium are both negative, providing negative values of the phase velocity and refraction index, among other peculiarities (Veselago, 1968). This first left-handed SRR-based CPW was inspired on the medium of Smith et al., 2000. By etching SRRs in the back substrate side of the CPW, beneath the slots, and shunt connected metallic strips between the central strip and ground plane. A one dimensional effective medium with simultaneous negative permeability (due to the presence of the SRRs) and permittivity (thanks to the shunt strips) in a narrow band was achieved (Martín et al., 2003).

The resonators used in this kind of transmission lines based on the resonant approach can be SRRs or other similar resonators with different topologies based on the SRR. The layout for the SRR is shown in Fig. 1(a). In Fig. 1, other examples of these resonators, like the spiral resonator (SR, Fig. 1b) with only one metal layer, are shown. Resonators implemented with two metal layers, like the broadside coupled non-bianisotropic split ring resonator (BC-NB-SRR, Fig. 1c), the broadside coupled spiral resonator with two turns (BC-SR(2), Fig. 1d) and the broadside coupled spiral resonator with four turns (BC-SR(4), Fig. 1e) are also depicted (Marqués et al., 2003; Aznar et al., 2008b).
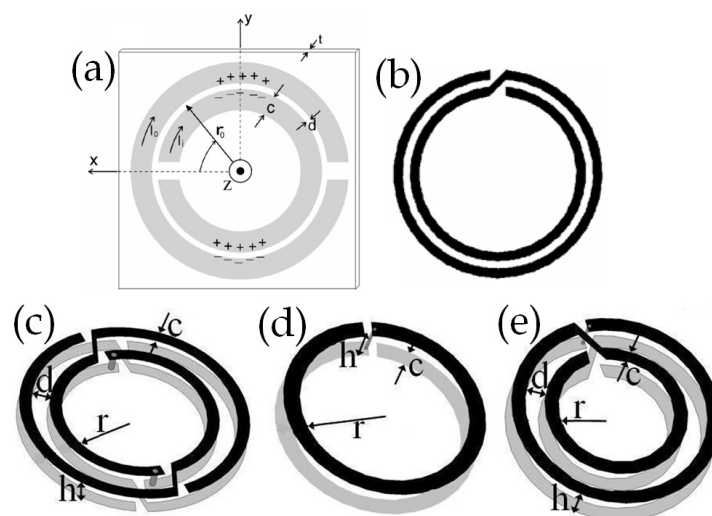

Fig. 1. Examples of topologies of different resonators based on the SRR (a): SR (b), BC-NB-SRR (c), BC-SR(2) (d) and BC-SR(4) (e).

The equivalent circuit model for the SRR is shown in Fig. 2(a) (Baena et al., 2005). The capacitance $C_0/2$ is related with each of the two SRR halves, whereas L_s is the resonator self-inductance. C_0 can be obtained as $C_0 = 2\pi r C_{pul}$, where C_{pul} represents the per unit length capacitance between de rings forming the resonator. Regarding L_s, it can be approximated to the inductance of a single ring with the average radius of the resonator and the width of the rings, c. Taking into account the circuit model of the resonator, its resonance frequency can be calculated as:

$$\omega_0 = \frac{1}{\sqrt{L_S C_S}}$$ (1)

The resonators based on the SRR, like the examples represented in Fig. 1 can also be modelled by a simple L-C resonant tank (see Fig. 2b). As long as the inductance and the

capacitance of the resonator can be increased (within the technology limits), the resonance frequency of the SRR can be decreased, reducing its electrical size (Aznar et al., 2008b). This is the case of the resonators shown in Fig. 1, which are electrically smaller than the SRR.
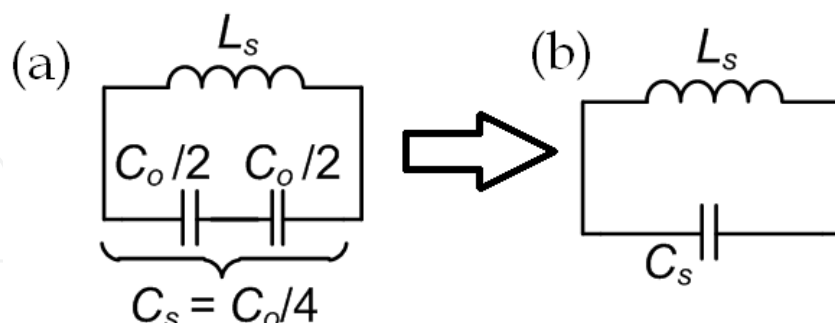

Fig. 2. Equivalent circuit models for a SRR (a) and simplified equivalent circuit model for a resonator based on SRR (b).
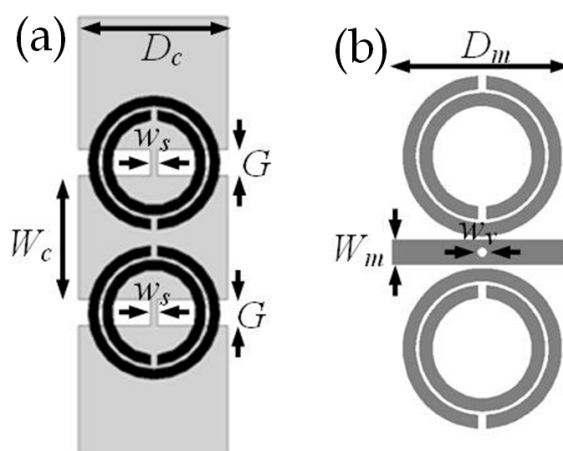

Fig. 3. Layouts of metamaterial transmission lines loaded with resonators based on SRR in CPW (a) and microstrip (b) technology.

The layout of two unit cells of metamaterial transmission lines loaded with resonators based on SRR are shown in Fig. 3(a) for CPW and Fig. 3(b) for microstrip technology. In the CPW configuration, the SRRs are paired on the lower substrate side (where they are etched), beneath the slots of the structure and centred with the shunt strips. The resonators are responsible for the negative effective permeability, whereas negative effective permittivity is achieved by means of the shunt connected strips. In case the shunt strips are eliminated, the CPW loaded with resonators provides only negative permeability, showing stop-band behaviour.

In the case of microstrip lines, the SRRs can be etched in pairs on the upper substrate side, adjacent to the conductor strip. The metallic vias are responsible for the negative permittivity of the structure in this case as well.

2.2 Transmission lines based on Complementary Split-Ring Resonators (CSRRs)

The layout of the CSRR is shown in Fig. 4(a). This resonator results from the application of the Babinet principle to the structure of the SRR, which leads to its complementary

counterpart (Falcone et al., 2004). In the CSRR the rings are etched on a metallic surface and its electric and magnetic properties are interchanged with respect to the SRR: the CSRR can be excited by an axial time-varying electric field and exhibits negative values of the dielectric permittivity.
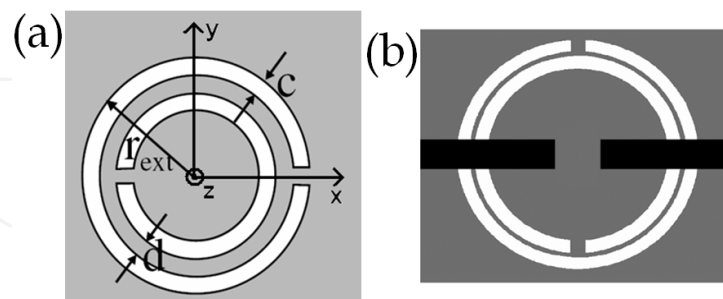

Fig. 4. (a) Representation of a complementary split ring resonator (CSRR); in this case the resonator is etched on a metallic surface; metallic part is represented in grey. (b) Scheme of a unit cell of a CSRR-based resonant-type metamaterial transmission line. CSRRs are etched on the ground plane (in grey) of a microstrip line just below the capacitive gaps etched on the signal strip (black).
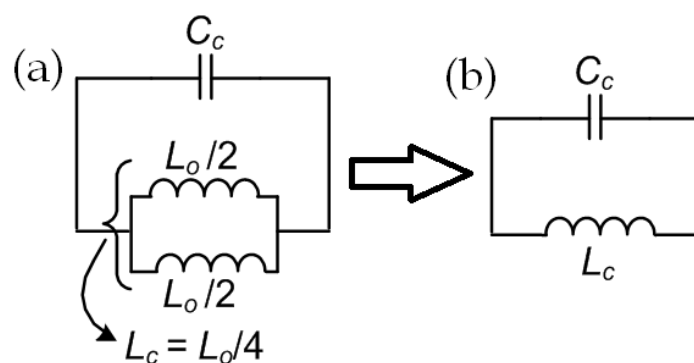

Fig. 5. Equivalent circuit models for a CSRR (a) and simplified equivalent circuit model for a resonator based on CSRR (b).

In this case, the CSRRs are etched on the ground plane of a microstrip transmission line. The CSRRs, which provide negative permittivity, are combined with capacitive gaps etched on the signal strip just above the resonators (see Fig. 4b). The gaps are in this case responsible for the negative permeability. The equivalent circuit model of the CSRR is shown in Fig. 5(a) (Baena et al., 2005). The resonance frequency of the CSRR is roughly the same of the frequency of a SRR with the same dimensions. Many other resonators admit a complementary counterpart, like, for example the SR shown in Fig. 1(b).

2.3 Transmission lines based on open resonators: Open Split-Ring Resonators (OSRRs) and Open Complementary Split-Ring Resonators (OSRRs)

A different kind of resonators consists in open resonators. Fig. 6 shows the layouts and equivalent circuit models of the open SRR (Martel et al., 2004) and the open complementary SRR (Vélez et al., 2009). As can be seen in the layout, the OSRR is based on the SRR and is obtained by truncating the rings forming the resonator and elongating them outwards. The OCSRR can be obtained as the complementary particle of the OSRR, in a similar way as the

CSRR is obtained from the SRR. These resonators, as is shown in Figs. 6 and 7, can be implemented either in microstrip or in coplanar technology (Aznar et al., 2008b, 2009a, 2009b; Durán-Sindreu et al., 2009; Vélez et al., 2010). The equivalent circuit models of the resonators are also shown in Fig. 6. The model of the OSRR is a series LC resonator (Martel et al., 2004). The inductance L_s can be obtained as the inductance of a ring with the average radius of the resonator and the same width, c, of the rings forming the OSRR. The capacitance C_0 is the distributed edge capacitance that appears between the two concentric rings. In a similar way, the OCSRR can be modelled by means of a parallel LC resonant tank (Aznar et al., 2008b; Vélez et al., 2009), where the inductance L_0 is the inductance of the metallic strip between the slot hooks and the capacitance is that of a disk with radius r_0-c/2 surrounded by a metallic plane separated by a distance c. According to this, it follows that, for identical dimensions and substrate, the resonance frequency of the OSRR or OCSRR is half the resonance frequency of the SRR or CSRR, respectively.
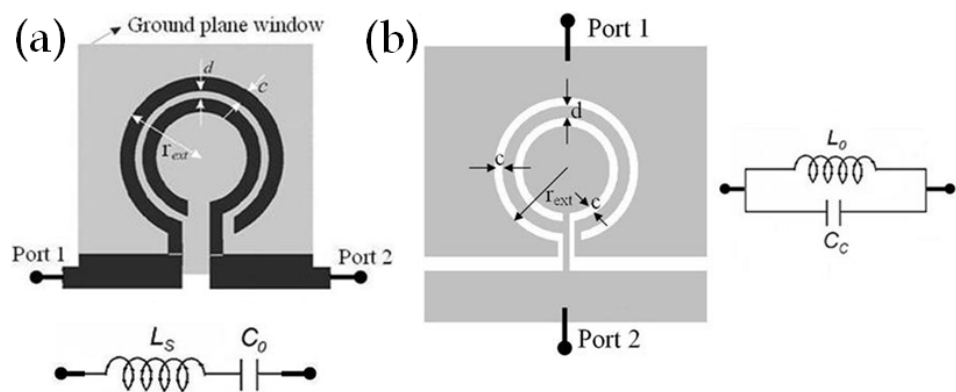

Fig. 6. Examples of microstrip structures loaded with open resonators. (a) Open split-ring resonator (OSRR) and its equivalent circuit model. (b) Open complementary split-ring resonator (OCSRR) and its equivalent circuit model.

As example, Fig. 7(a), shows a CPW transmission line loaded with a pair of OCSRRs. Fig. 7(b) represents an OSRR-based CPW unit cell.
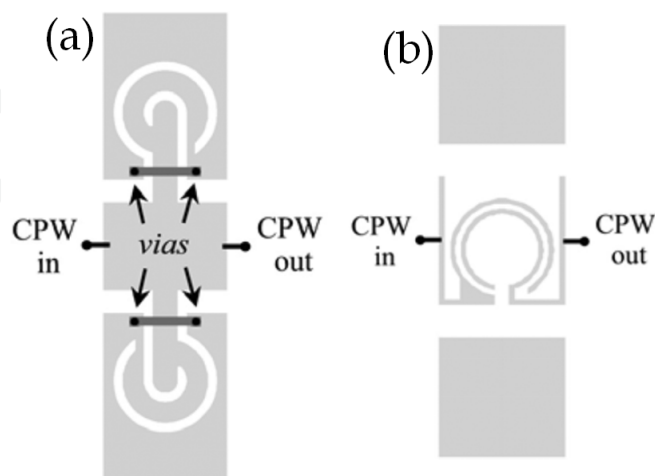

Fig. 7. Layout of a CPW based on OCSRR (a) and based on OSRR (b). In (a) the backside strips (in dark grey) connecting the different ground plane regions are necessary to prevent the slot mode of the CPW and the second resonance of the OCSRRs.

3. Equivalent circuit models for metamaterial transmission lines based on the resonant approach

In this section, we present the equivalent circuit models for the resonant-type metamaterial transmission lines presented in section 2. These models have been widely studied and confirmed and are able to model the composite behaviour of the considered structures (Aznar et al., 2008a; Gil et al., 2006). For a given kind of structure, the circuits are independent on the employed resonator. This means that the model for structures based on SRRs would be the same in case that the employed resonators were, for example, spiral resonators, which are electrically smaller but have the same equivalent circuit as the SRRs.

3.1 Equivalent circuit model for metamaterial transmission lines based on Split-Ring Resonators (SRRs)

The behaviour of the SRR-based structures (with and without shunt connected strips) can be interpreted to the light of the lumped element equivalent circuit models of the unit cells (Aznar et al., 2008a) (see Fig. 8a). Fig. 9 shows the typical behavior of two structures based on SRRs. The first one (left-handed) includes shunt strips, whereas the second one (negative-permeability) does not. In the circuit model, L and C account for the line inductance and capacitance, respectively, C_s and L_s model the SRR, M is the mutual inductive coupling between the line and the SRRs, and L_p is the inductance of the shunt strips (in case they are included). From the transmission line approach of metamaterials (Caloz & Itoh, 2005; Marqués et al., 2008), it follows that the structure exhibits left-handed wave propagation in those regions where the series reactance and shunt susceptance are negative, whereas in case they are positive, the propagation is conventional. According to this, the model in Fig. 8(a) perfectly explains the composite behavior of the structures shown in Fig. 3 (Aznar et al., 2008c). The inductance of the shunt inductive strips L_p is located between the two inductances ($L/2$) that model each line section, to the left and right of the position of the shunt strips. This reflects the location of the inductive strips. The resulting model is neither a π circuit nor a T circuit. Consequently, the transmission zero frequency and the frequency where the phase shift nulls cannot be directly obtained from it. It can be demonstrated that the model of Fig. 8(a) can be transformed to a π circuit, more convenient for its study and formally identical to that of Fig. 8(b) with modified parameters.
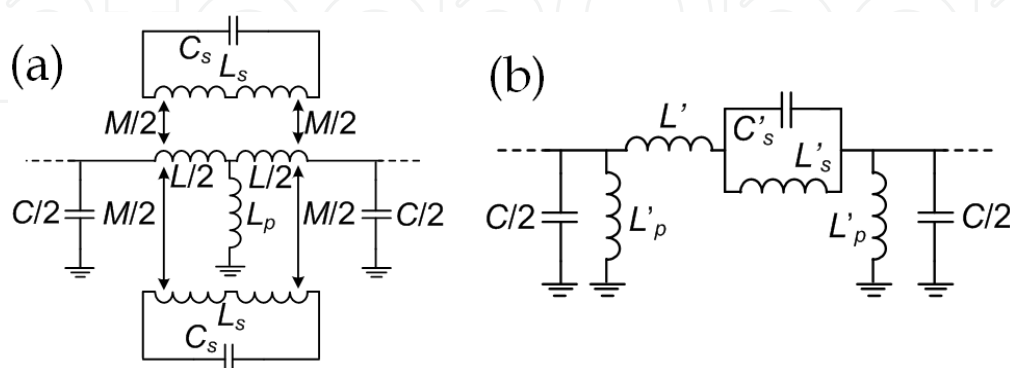

Fig. 8. Proposed circuit model for the basic cell of the left handed CPW or microstrip structure with loaded resonators based on the SRR (a). Transformation of the model to a π circuit (b).

Due to symmetry considerations and reciprocity, the admittance matrix of the circuit of Fig. 8(a) (which is a biport) must satisfy $Y_{12}=Y_{21}$ and $Y_{11}=Y_{22}$. From these matrix elements, the series (Z_s) and shunt (Z_p) impedances of the equivalent π-circuit model can be obtained (Pozar, 1990)

$$Z_S(\omega) = (Y_{21})^{-1} \tag{2}$$

$$Z_P(\omega) = (Y_{11} + Y_{21})^{-1} \tag{3}$$

Y_{21} is inferred by grounding port 1 and obtaining the ratio between the current at port 1 and the applied voltage at port 2. Y_{11} is simply the input admittance of the biport, seen from port 1, with a short circuit at port 2. After a straightforward but tedious calculation, the elements of the admittance matrix are obtained, and by applying Eq. 2 and Eq. 3, we finally obtain

$$Z_S(\omega) = j\omega\left(2 + \frac{L}{2L_P}\right)\left[\frac{L}{2} + M^2 \frac{1 + \frac{L}{4L_P}}{L_S\left(\frac{\omega_0^2}{\omega^2} - 1\right) - \frac{M^2}{2L_P}}\right] \tag{4}$$

$$Z_P(\omega) = j\omega\left(2L_P + \frac{L}{2}\right) \tag{5}$$

with $\omega_0 = (L_S C_S)^{-1/2}$. Expression 4 can be rewritten as

$$Z_S(\omega) = j\omega\left(2 + \frac{L}{2L_P}\right)\left[\frac{L}{2} + L'_S + \frac{L'_S}{1 - L'_S C'_S \omega^2}\right] \tag{6}$$

with

$$L'_S = 2M^2 C_S \omega_0^2 \frac{\left(1 + \frac{L}{4L_P}\right)^2}{1 + \frac{M^2}{2L_P L_S}} \tag{7}$$

$$C'_S = \frac{L_S}{2M^2 \omega_0^2}\left(\frac{1 + \frac{M^2}{2L_P L_S}}{1 + \frac{L}{4L_P}}\right)^2 \tag{8}$$

These results indicate that the circuit model of the unit cell of the left-handed lines loaded with SRRs and shunt inductors (Fig. 8a) can be formally expressed as the π circuit of Fig 8(b). These parameters are related to the parameters of the circuit of Fig. 8(a), according to Eq. 7, Eq. 8 and

$$L' = \left(2 + \frac{L}{2L_P}\right)\frac{L}{2} - L'_S \tag{9}$$

$$L'_P = 2L_P + \frac{L}{2} \tag{10}$$

The transmission zero frequency ω_z for the circuit of Fig. 8(a) can be obtained forcing $Z_S(\omega){=}\infty$. This gives

$$\omega_Z = \omega_0 \sqrt{\frac{1}{1 + \frac{M^2}{2L_P L_S}}} \tag{11}$$

It can be observed, that the transmission zero frequency is always located below the resonance frequency of the SRRs ω_0 ($\omega_z{<}\omega_0$). On the other hand, the frequency where $\phi{=}0$, ω_S, is obtained by forcing $Z_S(\omega){=}0$. This gives

$$\omega_S = \frac{1}{\sqrt{C_S\left(L_S - 2\frac{M^2}{L}\right)}} \tag{12}$$

Despite that $Z_S(\omega){=}0$ is a function of L_P, unexpectedly, ω_S does not depend on the shunt inductance.
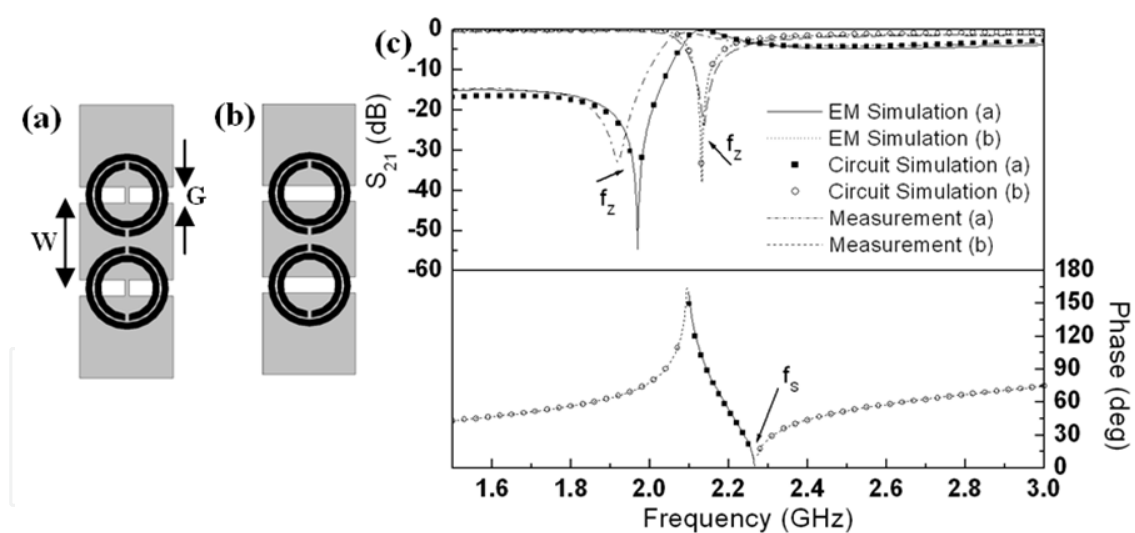

Fig. 9. Layouts of the considered CPW structures with SRRs and shunt strips (a) and with SRRs only (b); simulated and measured transmission coefficient S_{21} and simulated dispersion relation (c). The considered substrate is Rogers RO3010 with thickness h=1.27 mm and dielectric constant ε_r=10.2. Relevant dimensions are rings width c=0.6 mm, distance between the rings d=0.2 mm, and internal radius r=2.4 mm. For the CPW structure, the central strip width is W=7 mm and the width of the slots is G=1.35 mm. Finally, the shunt strip width is 0.2 mm. The results of the electrical simulation with extracted parameters are depicted by using symbols. We have actually represented the modulus of the phase since it is negative for the left-handed line. Discrepancy between measurement and simulation is attributed to fabrication related tolerances.

In Fig. 9 we can see two configuration examples for a CPW with loaded SRRs, with and without shunt strips. Electromagnetic simulation, circuit simulation and measurement show very good agreement in both cases. Therefore, we are able to confirm that the proposed circuit model is correct and accurate. This circuit model can also be applied to the microstrip structure shown in Fig. 3(b), which is in this sense, equivalent to the CPW structure.

3.2 Equivalent circuit model for metamaterial transmission lines based on Complementary Split-Ring Resonators (CSRRs)

The equivalent circuit model for the CSRR-based structure shown in Fig. 4(b) is the circuit shown in Fig. 10(a), which provides an accurate description of the behaviour of the structure (Aznar et al, 2008c, 2008d) and can be transformed into the circuit shown in Fig 10(b).
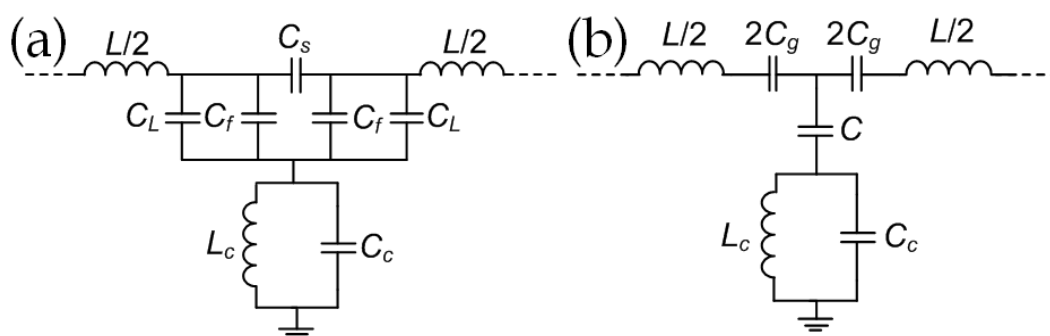

Fig. 10. Equivalent circuit model for the structure based on CSRR shown in Fig. 4(b) (a). Modified circuit model for the structure based on CSRR shown in Fig. 4(b) (b).

In the equivalent circuit (Fig. 10 a), the resonator is modelled by the resonant tank formed by L_c and C_c. The line parameters are L and C_L and the gap is modelled by the π-structure formed by C_s and C_f, which take into account the series and the fringing capacitances due to the presence of the capacitive gap. The modified circuit (Fig. 10b) is perfectly able to reproduce the behaviour of the structure. Nevertheless, the equivalent circuit (Fig. 10a) can be transformed into the modified circuit (Fig. 10b), by means of the following equations:

$$C_{par} = C_f + C_L \tag{13}$$

$$2C_g = 2C_s + C_{par} \tag{14}$$

$$C = \frac{C_{par}\left(2C_s + C_{par}\right)}{C_s} \tag{15}$$

so that the modified circuit (Fig. 10b), much simpler, can substitute the equivalent circuit (Fig. 10a) for a more straightforward work. The excellent agreement between electromagnetic and electrical simulation (employing the proposed model) can be observed in Fig. 11 (a). The notable frequencies (ω_z, ω_0) of this circuit model are indicated below in section 4.1.

In case the host transmission line is loaded just with CSRRs, the resulting structure shows negative permittivity and, thus, stop-band behaviour. This is the case of the structure shown

in Fig. 11 (b). For these structures, the circuit model would be the same as in Fig. 10(b) except for the capacitances C_g, which would be eliminated.
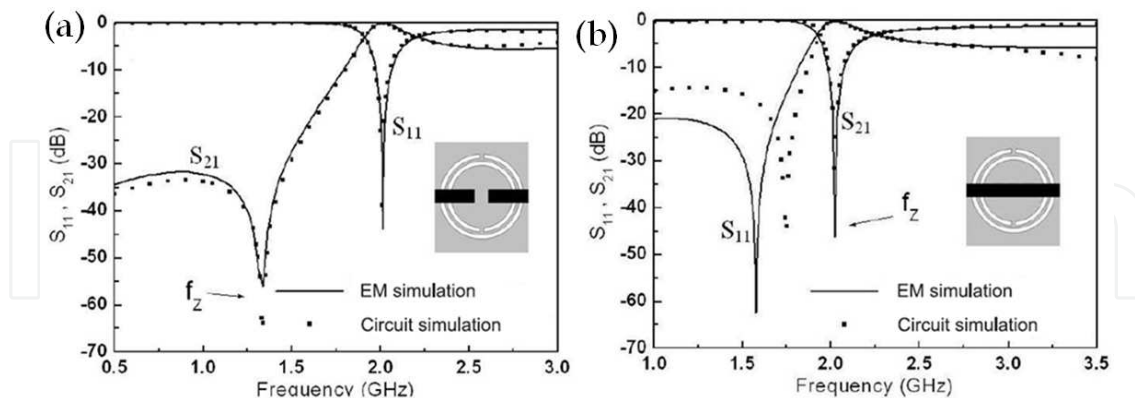

Fig. 11. Simulated (through the Agilent Momentum commercial software) frequency responses of the unit cell structures shown in the insets: (a) microstrip line loaded with CSRRs and series gaps, (b) microstrip line only loaded with CSRRs. The response that has been obtained from circuit simulation of the equivalent model with extracted parameters is also included. For the structures (a) and (b), the dimensions are: the strip line width W_m = 1.15 mm, the length D = 8 mm, and the gap width w_g = 0.16 mm. In both cases, the dimensions for the CSRR are: the outer ring width c_{out} = 0.364 mm, the inner ring width c_{inn} = 0.366 mm, distance between the rings d = 0.24 mm, and the internal radius r = 2.691 mm. The considered substrate is Rogers RO3010 with the dielectric constant ε_r = 10.2 and the thickness h = 1.27 mm.

3.3 Equivalent circuit models for metamaterial transmission lines based on open resonators: Open Split-Ring Resonators (OSRRs) and Open Complementary Split-Ring Resonators (OSRRs)

We will now consider the model of a CPW transmission line loaded with a pair of OCSRRs shown in Fig. 7(a). The resonator is represented by the elements C_p and L_p in Fig. 12(a). Although the particle is electrically small, it has been found that the structure exhibits certain frequency shift at resonance with respect to the frequency theoretically predicted by the equivalent circuit shown in Fig. 6. This frequency shift is expected if access lines are present. However, in the absence of access lines, we still obtain a small (although non negligible) phase shift. This means that the OCSRR-loaded CPW cannot be merely modeled as a two-port network with a shunt connected parallel resonator. To properly model the structure, we must introduce additional elements to account for the phase shift. That is, we must introduce phase shifting lines at both sides of the resonator. Such transmission line sections can be modeled through series inductances (L) and shunt capacitances (C), as depicted in Fig. 12(a). For design purposes, we can also use the simplified model depicted in Fig 12(b).

For a CPW loaded with a series connected OSRR represented in Fig. 7(b), a similar phenomenology results. Thus, to take into account these parasitic effects, we must introduce additional elements in the two port network describing the structure. A typical topology and the circuit model of these OSRR-loaded CPW transmission line sections are depicted in Fig. 12(c) and Fig. 12(d).
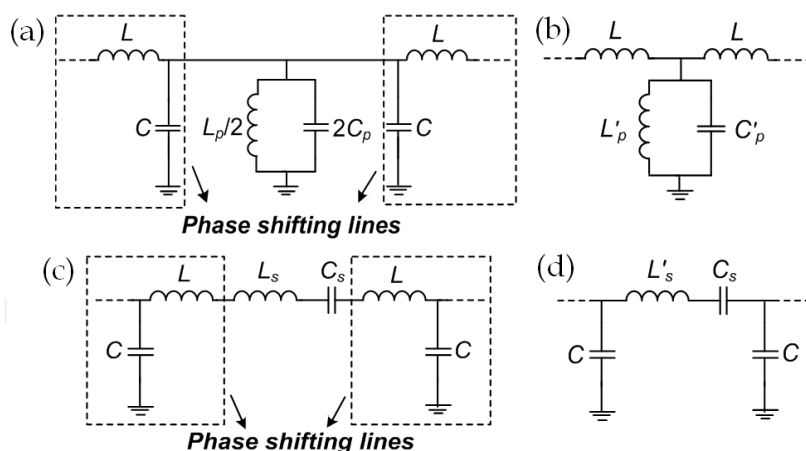
Fig. 12. (a) Circuit model, and (b) simplified circuit model of a CPW transmission line loaded with a pair of OCSRRs. (c) Circuit model, and (d) simplified circuit model of a CPW transmission line loaded with a series connected OSRR.

The transformation to simplify the circuit based on OSRR (Figs. 7b, 12 c and 12 d) is:

$$L'_S = L_S + 2L \tag{16}$$

and the transformations to simplify the circuit based on OCSRR (Figs. 7a, 12 a and 12 b) are:

$$C'_P = 2C_P + 2C \tag{17}$$

$$L'_P = \frac{L_P}{2} \tag{18}$$

4. Parameter extraction technique for metamaterial transmission lines based on the resonant approach

In previous sections we have presented different metamaterial transmission lines loaded with resonators and their equivalent circuit models. In this section we present a parameter extraction technique which, properly modified, can be applied to all of them. With this technique we can determinate the parameters of the circuit model of the structure. This represents an important assist in the design process, which becomes easier and faster.

The parameter extraction method consists in the imposition of several conditions obtained either from the simulated or measured response of the considered structure. The number of imposed conditions must be enough to obtain the values of all the parameters of the circuit.

4.1 Parameter extraction technique metamaterial transmission lines based on Split-Ring Resonators (SRRs)

The parameter extraction for the metamaterial transmission line based on SRRs is focused on the simplified equivalent circuit of the Fig. 8(b). This method was proposed in the reference (Aznar et al., 2008e). Since the number of parameters of the circuit model is five, we also need five conditions to univocally determine all parameters. From the representation of the reflection coefficient of a single unit cell, S_{11}, in the Smith chart, two

conditions are obtained. Firstly, we can determine the frequency that nulls the series reactance, f_s, from the intercept of S_{11} with the unit conductance circle (see Fig. 13 a). This is obvious since at this frequency, the real part of the admittance seen from the ports is simply the admittance of the opposite port, that is, $Y_0=(Z_0)^{-1}=(50\Omega)^{-1}=0.02$ S. Hence, S_{11} must be allocated in the unit conductance circle at f_s, as illustrated in the example provided in Fig. 13. This frequency is given by the following expression:

$$f_S = \frac{1}{2\pi}\sqrt{\frac{1}{L'_S C'} + \frac{1}{L' C'_S}} \tag{19}$$

Secondly, the susceptance of the unit cell seen from the ports at f_s, whose value can be inferred from the Smith chart, is

$$B(\omega_S) = \frac{C L'_P \omega_S^2 - 2}{L'_P \omega_S} \tag{20}$$

with $\omega_S = 2\pi f_S$. The next condition concerns the parallel resonator of the series branch. Namely, the resonance frequency of this resonator is given by

$$f_Z = \frac{1}{2\pi}\sqrt{\frac{1}{L'_S C'_S}} \tag{21}$$

Notice that this frequency does not coincide with the intrinsic resonance frequency of the magnetically driven resonator, f_o (which is the resonance frequency of the tank formed by L_s and C_s). The transmission zero frequency f_z (Eq. 21) can be easily obtained from the transmission coefficient S_{21} of the unit cell since at this frequency the series branch is opened and the whole power injected from the input port is reflected back to the source. Thus, the transmission coefficient nulls (zero transmission) and f_z can easily be identified from the representation of the transmission coefficient in a decibel scale (see example in Fig. 13 b).

Another condition can be deduced from the phase of the transmission coefficient, ϕ_{S21}. At the frequency where $\phi_{S21}=90^o$, $f_{\pi/2}$, the electrical length of the unit cell, $\phi=\beta l$ (β being the phase constant and l the length of the unit cell), is $\phi(f_{\pi/2}) = -90^o$. Since the dispersion relation of a periodic structure consisting of cascaded unit cells, as those in Fig. 8(b) is

$$\cos\phi = 1 + \frac{Z_S(\omega)}{Z_P(\omega)} \tag{22}$$

with Z_s and Z_p being the series and shunt impedances, respectively, of the π-circuit model, it follows that

$$Z_S(\omega_{\pi/2}) = -Z_P(\omega_{\pi/2}) \tag{23}$$

with $\omega_{\pi/2} = 2\pi f_{\pi/2}$. Expressions (19-21) and (23) are four of the five conditions needed to univocally determine the circuit parameters in Fig. 8(b). Now, by removing the shunt connected vias or strips in the layouts in Fig. 3, we can represent the corresponding

reflection coefficient on a Smith chart and read the susceptance seen from the ports at that frequency where S_{11} intercepts the unit conductance circle. Since this is simply the susceptance corresponding the line capacitance (provided L_p has been removed), we can thus univocally determine C. Hence, this is the fifth condition that is required to extract the circuit parameters of the circuit model in Fig. 8(b).
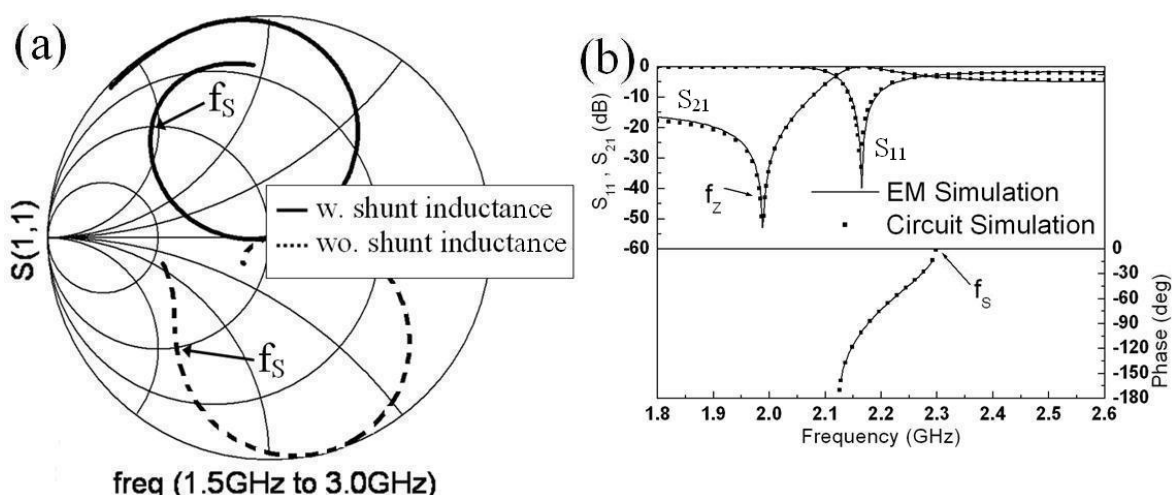

Fig. 13. Reflection coefficient on the Smith chart (a); frequency response (reflection, S_{11}, and transmission, S_{21}, coefficients) depicted in a decibel scale and the dispersion relation (b) for a left handed cell based on a CPW structure.

4.2 Parameter extraction technique metamaterial transmission lines based on Complementary Split-Ring Resonators (CSRRs)

The technique is based on the equivalent circuit model of a CSRR-loaded transmission line shown in Fig. 10(b). This method was proposed in 2006 (Bonache et al., 2006c). The considered structures are a negative permittivity as well as a left handed microstrip line (gap capacitors are required in the latter case). In view of the models, if losses are neglected (this is reasonable in a first order approximation), two characteristic frequencies can be identified: the frequency that nulls the shunt impedance (transmission zero frequency, f_z) and the frequency that nulls the shunt admittance (which obviously coincides with the intrinsic resonance frequency of the CSRR, f_0). These frequencies are given by the following expressions:

$$f_Z = \frac{1}{2\pi\sqrt{L_C(C + C_c)}} \tag{24}$$

$$f_0 = \frac{1}{2\pi\sqrt{L_C C_C}} \tag{25}$$

and they can be either experimentally determined, or obtained from the simulated response of the structure. At f_z a notch in the transmission coefficient is expected and this frequency can be accurately measured. To obtain f_0, a representation of the transmission coefficient on a Smith chart is required (see example in Fig. 14). At this frequency the shunt path to ground

is opened, and the input impedance seen from the ports is solely formed by the series elements of the structure (*L*, for the negative permittivity line, and *L* and C_g for the left handed line) and the resistance of the opposite port (50 Ω). Therefore, f_0 is given by the intersection between the measured (or simulated) S_{11} curve and the unit normalized resistance circle. From this result we can also obtain the impedance of the series elements at that frequency. This gives directly the value of *L* for the negative permittivity line. For the left handed line, *L* can be independently estimated from a transmission line calculator, or from the value extracted for the negative permeability line, corrected by the presence of the gap, whereas C_g can be determined by adjusting its value to fit the impedance value read from the Smith chart at f_0 from the simulation or experiment.
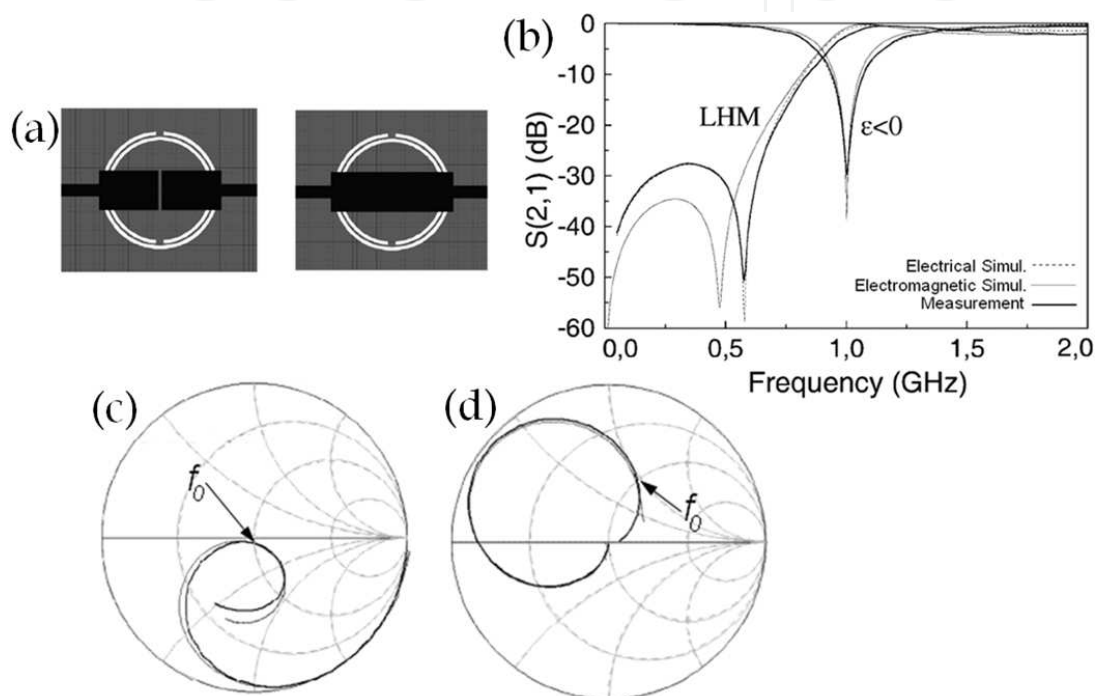

Fig. 14. (a) Layouts of the structures employed in the parameter extraction method for the CSRR-based unit cell. (b) Frequency responses of the measurement, the electromagnetic simulation and the electric simulation employing the extracted parameters. Representation of the S$_{11}$ parameter for the identification of the CSRR resonance frequency (c) for the complete (LH) structure (d) for the structure without gap (ε<0). Measurement and electric simulation.

Expressions (24) and (25) are dependent on three parameters. Therefore, we cannot directly obtain the element values of the CSRR (as desired) and the coupling capacitance. To this end, we need an additional condition, namely:

$$Z_S\left(j\omega_{\pi/2}\right) = -Z_P\left(j\omega_{\pi/2}\right) \tag{26}$$

where $Z_S\left(j\omega\right)$ and $Z_P\left(j\omega\right)$ are the series and shunt impedance of the T-circuit model of the structure, respectively, and $\omega_{\pi/2}$ is the angular frequency where the phase of the transmission coefficient (which is a measurable quantity) is $\phi\left(S_{21}\right) = \pi/2$. Thus, from (23)–(25) we can determine the three reactive element values that contribute to the shunt impedance.

4.3 Parameter extraction technique for metamaterial transmission lines based on open resonators: Open Split-Ring Resonators (OSRRs) and Open Complementary Split-Ring Resonators (OSRRs)

This subsection is focused on the parameter extraction for the structures represented in Fig. 7. The parameters of the circuit model of a CPW loaded with an OSRR (Fig. 12 d) can be extracted from the measurement or the electromagnetic simulation of the structure following a straightforward procedure (Durán-Sindreu et al., 2009a, 2009b). First of all, from the intercept of the return loss curve with the unit conductance circle in the Smith chart, we can directly infer the value of the shunt capacitance according to

$$C = \frac{B}{2\omega_{Z_S=0}} \tag{27}$$

where B is the susceptance in the intercept point. The frequency at this intercept point is the resonance frequency of the series branch

$$\omega^2\big|_{Z_S=0} = \frac{1}{C_S L_S'} \tag{28}$$

To determine the other two element values of this branch, one more condition is needed. This condition comes from the fact that at the reflection zero frequency ω_z (maximum transmission) the characteristic impedance of the structure is 50Ω. In this π-circuit, the characteristic impedance is given by

$$Z_0(\omega) = \sqrt{\frac{Z_P(\omega)^2 Z_S(\omega)}{2Z_P(\omega) + Z_S(\omega)}} \tag{29}$$

Thus, by forcing this impedance to 50Ω, the second condition results. By inverting (27) and (28), we can determine the element values of the series branch. The following results are obtained:

$$C_S = \left[\frac{\omega_Z^2}{\omega^2\big|_{Z_S=0}} - 1\right]\left\{\frac{1}{2Z_0^2 \omega_Z^2 C} + \frac{C}{2}\right\} \tag{30}$$

$$L_S' = \frac{1}{\omega^2\big|_{Z_S=0} C_S'} \tag{31}$$

The parameters of the circuit model of a CPW loaded with an OCSRR (Fig. 12 b) can be extracted following a similar procedure. In this case, the intercept of the return loss curve with the unit resistance circle in the Smith chart gives the value of the series inductance

$$L = \frac{X}{2\omega\big|_{Z_P\to\infty}} \tag{32}$$

where X is the reactance at the intercept point. The shunt branch resonates at this frequency, that is,

$$\omega^2\Big|_{Z_P \to \infty} = \frac{1}{L'_P C'_P} \tag{33}$$

Finally, at the reflection zero frequency (ω_z), the characteristic impedance, given by

$$Z_0(\omega) = \sqrt{Z_S(\omega)\big[Z_S(\omega) + 2Z_P(\omega)\big]} \tag{34}$$

must be forced to be 50Ω. From these two latter conditions, we finally obtain

$$L'_P = \left[\frac{\omega_Z^2}{\omega^2\big|_{Z_P \to \infty}} - 1\right]\left\{\frac{Z_0^2}{2\omega_Z^2 L} + \frac{L}{2}\right\} \tag{35}$$

$$C'_P = \frac{1}{\omega\big|_{Z_P \to \infty} L'_P} \tag{36}$$

and the element values are determined.

5. Conclusion

In this chapter, different kinds of resonant-type metamaterial transmission lines based on subwavelength resonators have been presented and studied. There are several types of resonators which allow their use in the implementation of this kind of artificial transmission lines. SRR-, CSRR- and open resonator-based structures have been presented and studied. The equivalent circuit models for each of the kinds of structures presented have been exposed, together with their parameter extraction methods. These methods provide the circuit model parameters, extracted from the frequency response of the structure, being a very useful design tool and allowing the corroboration of the proposed circuits as correct models for the considered structures. Furthermore, thanks to their accuracy, the parameter extraction methods have already been applied in automation procedures which allow the automatic generation of layouts for this kind of structures (Selga et al., 2010). After the imposition of certain conditions on the frequency response, which implies certain values for the circuit model parameters, the layout of the structure satisfying the required conditions can be automatically generated by means of space mapping techniques. This is a good example of the usefulness and importance of the equivalent circuit models and the parameter extraction methods.

6. References

Aznar, F.; Bonache, J. & Martín, F., Improved circuit model for left-handed lines loaded with split ring resonators, *Applied Physics Letters*, vol. 92, February 2008, pp. 043512-3, ISSN 0003-6951.

Aznar, F.; García-García, J.; Gil, M.; Bonache J. & Martín, F. Strategies for the miniaturization of metamaterial resonators, *Microwave and Optical Technology Letters*, vol. 50, May 2008, pp. 1263-1270, ISSN 1098-2760.

Aznar, F.; Gil, M.; Bonache J. & Martín, F., Revising the equivalent circuit models of resonant-type metamaterial transmission lines, *Proceedings of the IEEE MTT-S Int'l Microwave Symposium*, pp. 323-326, ISBN: 978-1-4244-1780-3 Atlanta (USA), June 2008.

Aznar, F.; Gil, M.; Bonache, J. & Martín, Modelling metamaterial transmission lines: a review and recent developments, *Opto-Electronics Review*, vol. 16, September 2008, pp. 226-236, ISSN 1230-3402.

Aznar, F.; Gil, M.; Bonache, J.; Jelinek, L.; Baena, J. D.; Marqués, R. & F. Martín, Characterization of miniaturized metamaterial resonators coupled to planar transmission lines through parameter extraction, *Journal of Applied Physics*, Vol 104, December 2008, 114501, ISSN 0021-4922.

Aznar, F.; Vélez, A.; Bonache, J.; Menés J. & Martín, F. Compact lowpass filters with very sharp transition bands based on open complementary split ring resonators, *Electronics Letters*, Vol. 45, No. 6, March 2009, pp. 316-317, ISSN 0013-5194.

Aznar, F.; Vélez, A.; Durán-Sindreu, M.; Bonache J. & Martín, F., Elliptic-function CPW low-pass filters implemented by means of open complementary split ring resonators (OCSRRs, *IEEE Microwave and Wireless Components Letters*, vol. 19, November 2009, pp. 689-691, ISSN 1531-1309.

Aznar, F.; Vélez, A.; Durán-Sindreu, M.; Bonache J. & Martín, F., Open complementary split ring resonators: physics, modelling, and analysis, *Microwave and Optical Technology Letters*, vol. 52, July 2010, pp. 1520-1526, ISSN 1098-2760.

Baena, J. D.; Bonache, J.; Martín F.; Sillero, R. M.; Falcone, F.; Lopetegi, T.; Laso, M. A. G.; García-García, J.; Gil, I.; Portillo, M. F. & Sorolla, M. Equivalent-circuit models for split-ring resonators and complementary split-ring resonators coupled to planar transmission lines, *IEEE Transactions on Microwave Theory and Techniques*, vol. 53, April 2005, pp. 1451-1461, ISSN 0018-9480.

Bonache, J.; Gil, I.; García-García, J. & Martín, F. Novel microstrip band pass filters based on complementary split rings resonators, *IEEE Transactions on Microwave Theory and Techniques*, vol. 54, January 2006, pp. 265-271, ISSN 0018-9480.

Bonache, J.; Martel, J.; Gil, I.; Gil, M.; García-García, J.; Martín, F.; Cairó, I. & Ikeda, M. Super compact (<1cm2) band pass filters with wide bandwidth and high selectivity at C-band, *Proceedings of the 36th European Microwave Conference*, pp. 599-602, ISBN 2-9600551-6-0, Manchester, UK, September 2006.

Bonache, J.; Gil, M.; Gil, I.; Garcia-García, J. & Martín, F., On the electrical characteristics of complementary metamaterial resonators, *IEEE Microwave and Wireless Components Letters*, vol. 16, October 2006, pp. 543.545, ISSN 1531-1309.

Caloz, C. & Itoh, T. (2005). *Electromagnetic Metamaterials: Transmission Line Theory and Microwave Applications*, Wiley Interscience, ISBN 978-0-471-66985-2.

Durán-Sindreu, M.; Aznar, F.; Vélez, A.; Bonache, J. & Martín, F. New composite, Right/Left handed transmission lines based on electrically small, open resonators, *Proceedings of IEEE MTT-S International Microwave Symposium*, pp. 45-48, ISBN 978-1-4244-2804-5, Boston (MA), USA, June 2009.

Durán-Sindreu, M.; Vélez, A.; Aznar, F.; Sisó, G; Bonache, J. & Martín, F., Application of open split ring resonators and open complementary split ring resonators to the synthesis of artificial transmission lines and microwave passive components, *IEEE Transactions on Microwave Theory and Techniques*, vol. 57, December 2009, pp. 3395-3403, ISSN 0018-9480.

Falcone, F.; Lopetegi, T.; Laso, M. A. G.; Baena, J. D.; Bonache, J.; Beruete, M.; Marqués, R.; Martín, F. & Sorolla, M. Babinet principle applied to the design of metasurfaces and metamaterials, *Physical Review Letters*, vol. 93, November 2004, 197401, ISSN 1079-7114.

Gil, M.; Bonache, J.; Gil, I.; García-García, J. & Martín, F., On the transmission properties of left handed microstrip lines implemented by complementary split rings resonators, *Int. Journal Numerical Modelling: Electronic Networks, Devices and Fields*, vol. 19, March 2006 , pp 87-103, ISSN 0894-3370.

Gil, M.; Bonache, J.; Gil, I.; García-García, J. & Martín, F., Miniaturization of planar microwave circuits by using resonant-type left handed transmission lines, *IET Microwave Antennas and Propagation*, Vol.1, February 2007, pp. 73-79, ISSN 1751-8725.

Gil, M.; Bonache, J.; García-García, J.; Martel, J. & Martín, F. Composite right/left-handed metamaterial transmission lines based on complementary split-rings resonators and their applications to very wideband and compact filter design", *IEEE Transactions on Microwave Theory and Techniques*, Vol. 55, No. 6, June 2007, pp. 1296-1304, ISSN 0018-9480.

Martel, J.; Marqués, R.; Falcone, F.; Baena, J. D.; Medina, F.; Martín F. & Sorolla, M. A new LC series element for compact bandpass filter design, *IEEE Microwave and Wireless Components Letters*, vol. 14, May 2004, pp. 210-212, ISSN 1531-1309.

Marqués, R.; Mesa, F.; Martel, J. & Medina, F. Comparative analysis of edge- and broadside-coupled split ring resonators for metamaterial design - Theory and experiments, *IEEE Transactions on Antennas and Propagation*, vol. 51, October 2003, pp. 2572-2581, ISSN 0018-926X.

Marqués, R.; Martín, F. & Sorolla, M. (2008). *Metamaterials with Negative Parameters*, John Wiley & Sons, Inc., ISBN 978-0-471-74582-2.

Martín, F.; Bonache, J.; Falcone, F.; Sorolla M. & Marqués, R. Split ring resonator-based left-handed coplanar waveguide, *Applied Physics Letters*, vol. 83, December 2003, pp. 4652-4654., ISSN 0003-6951.

Pozar, M, (1990). *Microwave engineering*, Addison Wesley, ISBN 978-0-471-44878-5.

Selga, J; Rodríguez, A.; Gil, M.; Carbonel, J.; Voria, V.E. & Martín, F., Towards the automatic layout synthesis in resonant-type metamaterial transmission lines, *IET Microwave Antennas and Propagation*, Vol.4, August 2010, pp. 1007-1015, ISSN 1751-8725.

Sisó, G.; Gil, M.; Aznar, F.; Bonache, J. & Martín, F. Generalized Model for Multiband Metamaterial Transmission Lines, *IEEE Microwave and Wireless Components Letters*, Vol. 18, Num. 11, November 2008, pp 728-730, ISSN 1531-1309.

Sisó, G.; Gil, M.; Aznar, F.; Bonache, J. & Martín, F. Dispersion engineering with resonant-type metamaterial transmission lines, *Laser & Photonics Review*, vol. 3, Issue 1-2, February 2009, pp. 12-29, ISSN 1863-8880.

Smith, D. R.; Padilla, W. J.; Vier, D. C.; Nemat-Nasser S. C. & Schultz, S. Composite medium with simultaneously negative permeability and permittivity, *Physical Review Letters*, vol. 84, May 2000, pp. 4184-4187, ISSN 0031-9007.

Vélez, A.; Aznar, F.; Bonache, J.; Velázquez-Ahumada, M. C.; Martel J. & Martín, F. Open complementary split ring resonators (OCSRRS) and their application to wideband cpw band pass filters, *IEEE Microwave and Wireless Components Letters*, vol. 19, April 2009, pp. 197-199, ISSN 1531-1309.

Vélez, A.; Aznar, F.; Durán-Sindreu, M.; Bonache, J. & Martín, F., Stop-band and band-pass filters in coplanar waveguide technology implemented by means of electrically small metamaterial-inspired open resonators, *IET Microwave Antennas and Propagation*, Vol.4, June 2010, pp. 712-716, ISSN 1751-8725.

Veselago, V. G. The electrodynamics of substances with simultaneously negative values of ε and μ, *Soviet Physics Uspekhi*, January 1968, pp. 509-514, ISSN 0038-5670.

Metamaterial

Edited by Dr. Xun-Ya Jiang

In-depth analysis of the theory, properties and description of the most potential technological applications of metamaterials for the realization of novel devices such as subwavelength lenses, invisibility cloaks, dipole and reflector antennas, high frequency telecommunications, new designs of bandpass filters, absorbers and concentrators of EM waves etc. In order to create a new devices it is necessary to know the main electrodynamical characteristics of metamaterial structures on the basis of which the device is supposed to be created. The electromagnetic wave scattering surfaces built with metamaterials are primarily based on the ability of metamaterials to control the surrounded electromagnetic fields by varying their permeability and permittivity characteristics. The book covers some solutions for microwave wavelength scales as well as exploitation of nanoscale EM wavelength such as visible specter using recent advances of nanotechnology, for instance in the field of nanowires, nanopolymers, carbon nanotubes and graphene. Metamaterial is suitable for scholars from extremely large scientific domain and therefore given to engineers, scientists, graduates and other interested professionals from photonics to nanoscience and from material science to antenna engineering as a comprehensive reference on this artificial materials of tomorrow.

How to reference

In order to correctly reference this scholarly work, feel free to copy and paste the following:

INTECH
open science | open minds